CLASSIFICATION AND ANALYSIS OF DIGITAL MODULATION SCHEMES USING WIGNER-VILLE DISTRIBUTION

Nazan TUĞBAY and Bülent SANKUR

TÜBİTAK-Marmara Research Institute, Gebze, Kocaeli, Turkey
Istanbul Technical University, Istanbul, Turkey

RESUME

La Distribution Wigner-Ville a ete utilisee comme un moyen de classification et d' analyse des methodes de modulation numerique. On a calcule ces distributions dans les cas de PAM et CPFSK en utilisant les representations complexes en bande fondamentale. Les reliefs de temps-frequence des signaux a modulation numerique montrent des dependences marques en ce qui concerne le type de modulation ainsi que sur ses parametres. Ces reliefs ont ete parametre avec les fonctions Haar et un nombre limite de coefficients Haar ont ete trouve suffisants pour mettre en oeuvre une classification du type de modulation.

SUMMARY

The Wigner-Ville Distribution has been investigated as a tool for the classification and analysis of digital modulation schemes. Starting form the complex baseband representation of modulations, the WVD of PAM and CPFSK have been derived. The time-frequency reliefs of digitally modulated signals show strong dependencies on the type of modulation and upon the modulation parameters for a specific type. These reliefs have been further parametrized through Haar functions and it has been found out that a few Haar coefficients provide significant features for the recognition of the type of modulation.

I. INTRODUCTION

A modulation recognizer is a device for automatic recognition of modulation type of a signal. The information on modulation type of a signal serves as a parameter in signal sorting activities. For example, combined with other parameters such as the signal strength and the angle of arrival the output of each emitter can be catalogued, which in turn may start a series of control functions. Typical applications for modulation recognition and signal classification arise in surveillance, monitoring and reconnaissance of threats in the military context.

A classification algorithm must be based on stochastic models of modulated signals and their easily quantifiable parameters. Modulated signal processes are not however inherently stationary, since sampling and modulation operations induce cyclostationary behavior. Stationary models with time-invariant parameters cannot provide an exact representation of such processes. Time frequency representations with some time dependent probabilistic parameters can therefore provide more detailed information on the evolution of time-frequency reliefs, on the instantaneous frequency and group delay characteristics and on the hidden periodicities.

In this study the Wigner-Ville Distribution (WVD) is used as a joint time-frequency representation to gain insight into digital modulation types, such as PAM and CPFSK and to obtain an automatic recognition algorithm based on the parametrization of the time-frequency reliefs.

II. PROPERTIES of WVD

The WVD of a stochastic process x(t) with sample function X(t) is defined as [1]:

$$W_x(t,f)=E\{W_x(t,f)\}=\int_{-\infty}^{\infty} E\{X(t+\tau/2)X^*(t-\tau/2)\}\exp(-i2\pi f\tau)d\tau$$

Several requirements can be imposed on the definition of a joint time-frequency representation [2], such as realness, positivity, shift-invariance both with respect to time and frequency, preservation of the time and frequency supports, effects of linear systems that result in convolution type relationships, time and frequency profiles of the relief that match, respectively, the magnitude square and the power spectrum of the signal etc.. Although there exist several definitions of joint time-frequency reliefs, the WVD is the most consistent one in that it satisfies the largest number of properties provided the positivity constraint is relaxed. Although one thus foregoes pointwise energy interpretation, strictly non-negative values can be obtained by integrating the reliefs over an uncertainty ellipse. In the respect the WVD has the smallest uncertainty ellipse.

In the context of modulation study, the two relevant properties of WVD are given below:

a) Under time-shifting and modulation operations, the WVD is, respectively, time and frequency shifted, i.e., for $x(t-t_o)\exp(i2\pi f_o t)$, one has $W_x(t-t_o,f-f_o)$. As a consequence, in the study of modulation schemes, it will suffice to consider only the complex baseband signal.

b) If a signal has a finite time-bandwidth or finite frequency bandwidth, then the WVD is also confined to the same support, i.e., if

$x(t)=0 \quad t\notin T$ then $W_x(t,f)=0$ for $t\notin T$

$X(f)=0 \quad t\notin B$ then $W_x(t,f)=0$ for $f\notin B$

Thus it will suffice to confine the reliefs to a symbol interval.

III. WVD of DIGITAL MODULATION PROCESSES

It is conjectured that the time-frequency representations obtained through WVD of digitally modulated processes will be a usefull tool for the study of bandpass nonlinearities, for the extraction of timing information and for the identification of features for the differentiation between modulation types.

It will be convenient to represent the output of a modulator as

$$s(t)=\mathrm{Re}\{u(t)\exp(i2\pi f_c t)\}$$

where s(t) is the bandpass modulated signal and u(t) is the complex baseband modulating waveform. It is possible to accommadate all digital modulation types in this formalism [4]. For example for PAM (pulse amplitude modulation) one has

$$u(t)=\sum_n I_n g(t-nT)$$

where I_n is the information sequence, T is the symbol period and g(t) is the basic pulse waveform; for the case of CPFSK (continuous phase frequency shift keying) one has

$$u(t)=\sum_{n=0}^{\infty}\exp[j\phi+jw_d(\alpha_n T+(t-nT)I_n)]\,g(t-nT)$$

where ϕ is a uniformly distributed initial phase of the carrier, f_d is called the peak frequency deviation, g(t) is a rectangular pulse and $\alpha_n=\sum_{k=0}^{n-1} I_k$ representing the accumulation of all symbols up to time (n-1)T.

It should be pointed out that digitally modulated signals are cyclostationary processes with symbol period T, that is, their autocorrelation functions are periodic, $R_x(t,u)=R_x(t+T,u+T)$. The WVD reflects this cyclostationary nature, in that it becomes periodic in t when the input is a cyclostationary signal.

WVD of PAM:

For the PAM signal represented as $x(t)=I_n g(t-nT)$ where $\{I_n\}$ is a wide-sense stationary sequence with autocorrelation function $\gamma_I(n-m)$ the WVD becomes

$$W_x(t,f)=\sum_n\sum_m \gamma_I(n-m)\int g(t+\tau/2-nT)g^*(t-\tau/2-mT)\exp(-i2\pi f\tau)d\tau$$

which becomes

$$W_x(t,f)=0.5[\phi_I(f)-\phi_I(f-\tfrac{1}{2T})][W_g(t-\tfrac{T}{2},f)+W_g(t+\tfrac{T}{2},f)]$$

$$+0.5[\phi_I(f)+\phi_I(f-\tfrac{1}{2T})]W_g(t,f)$$

where $\phi_I(f)$ is the power spectral density of the sequence $\{I_n\}$. For the case of binary symmetric signalling (BSS), i.e., $I_n=\pm 1$ each with probability 1/2, the WVD of PAM reduces to the WVD of the pulse waveform, i.e., $W_x(t,f)=W_g(t,f)$, $|t|<T/2$ and the results for the on-off signalling (OOS), i.e., $I_n=0$ and 1 each with probability 1/2, are illustrated in Fig.2. Fig.1 displays the WVD of PAM with BSS and pulse duration d=T/2 in the time-frequency plane $|f|<4/T$ and $-0.5T<t<1.5T$. One can notice the periodic nature of WVD; also that the energy distribution evolves in time with a peak at DC frequency. Fig.2 illustrates the WVD of PAM with OOS which shows ridges along $f=\pm k/2T$, which may be potentially used to extract timing information. Notice that the ridges along the time direction toward the two ends of the signalling interval become negative; since positivity can not be guaranteed for the WVD. The isoplanars for the first relief is shown in Fig.3 which indicates a distinct orientation of the contours along the frequency axis centered at $t=kT$.

WVD of CPFSK:

The WVD of CPFSK can be calculated starting from

$$W_x(t,f) = \int_{-\infty}^{\infty} r_x(t,\tau)\exp(-i2\pi f\tau)d\tau$$

where

$$r_x(t,\tau) = \sum_{n=0}^{\infty} r_{n,n}(t,\tau)g(t+\frac{\tau}{2}-nT)g^*(t-\frac{\tau}{2}-nT)$$

$$+ \sum_{n=1}^{\infty}\sum_{m=0}^{n-1} r_{n,m}(t,\tau)g(t+\frac{\tau}{2}-nT)g^*(t-\frac{\tau}{2}-mT)$$

$$+ \sum_{m=1}^{\infty}\sum_{n=0}^{m-1} r_{n,m}(t,\tau)g(t+\frac{\tau}{2}-nT)g^*(t-\frac{\tau}{2}-mT)$$

where

$$r_{n,m}(t,\tau)=E\{\exp(jw_d(\alpha_n-\alpha_m)T)\exp[jw_d((t+\frac{\tau}{2}-nT)I_n - (t-\frac{\tau}{2}-mT)I_n)]\}$$

and for $t\in[KT,(K+1)T]$ can be expressed as

$$W_x(t,f) = \int_{-\infty}^{\infty} W_g(t-KT,u)\phi(f-u)du + 2Re\{A(K,f)B(K,t+\frac{T}{2}) + \phi(T)e^{-j2\pi fT}A(K,f)B(K,t)+A(K+1,f)B(K,t-\frac{T}{2})\}$$

where

$$\psi(\tau) = E\{e^{jw_d\tau I_n}\} \quad \text{and} \quad \phi(u) = \int_{-\infty}^{\infty}\psi(\tau)e^{-j2\pi f\tau}d\tau$$

$$A(K,f) = [\phi^{2K}(T)e^{-j2\pi fT(2K)}-1] / [\phi^2(T)e^{-j4\pi fT}-1]$$

$$B(K,t) = \int_{-\infty}^{\infty} W_g(t-KT,u)W_\phi(t-KT-\frac{T}{2},f-u)e^{-j2\pi uT}du$$

Figures 4-7 illustrate respectively, the reliefs and isoplanars for binary CPFSK with h=0.3 and h=0.7 ($h=2\pi f_d T$). It can be seen that these isoplanars show symmetry along the t-axis in contrast to the PAM case. Furthermore the reliefs show substantial changes with varying h parameter. For example, the persistent ridge for all time along the center frequency is evident especially for the small deviation case. For larger h values, e.g., h=0.7 the frequency sidelobes become prominent and the interference terms cause various undulations on the relief.

IV. AUTOMATIC MODULATION RECOGNITION

The reliefs and isoplanars shown in Figs. 1 to 7 display localized lobes and predictable orientation. Hear functions have been chosen to parametrize these reliefs to obtain significant features and to implement modulation recognition. Haar functions have in fact the ability to represent a given function with few constituent terms to a high degree of accuracy and they have been successfully applied to picture data compression. In particular one can note that (H(i,j),i,j=1,...,N, representing the (i,j)th Haar coefficient):

i) H(1,1) gives the total signal energy in the signalling interval T.

ii) H(1,i)'s and H(i,1)'s are sensitive to symmetries respectively in f and t.

iii) As a result of (ii), the differences in the orientation of the WVD contours of PAM and CPFSK can be quantitatively described by the Haar coefficients H(1,i) and H(i,1), i=1,...,N. In Table 1, this can be seen comparing the normalized Haar coefficients H(1,4), H(4,1), H(1,7) and H(7,1) of PAM and CPFSK.

iv) H(i,1), e.g., i=3 or 4 can detect the lobes along the frequency direction, as occur in CPFSK. The strong variation of Haar coefficients with the h-parameter as in Fig.8 is also an indication that these coefficients can be used to estimate the frequency deviation parameter in CPFSK.

Figures 9-11 display the Haar coefficients H(i,j), i,j=1,...,8 obtained from the WVD of PAM and CPFSK with h=0.3 and h=0.7.

IV. CONCLUSION

Preliminary studies have shown that the Wigner-Ville reliefs of digitally modulated signals show substantial dependence upon the type of modulation and upon the modulation parameters for a specific type. This dependence has been used as the basis for modulation type recognition by using two dimensional Haar functions as features. PAM with symmetric and on-off pulsing and CPFSK with various values of h have been classified by using a few Haar coefficients, e.g., H(1,4), H(4,1). It remains to study the performance of this digital modulation classifier under noisy conditions and to consider as well practical implementation aspects, such obtaining Haar feature vectors directly from measured signal.

REFERENCES

1. P. Flandrin, "Time-Dependent Spectra of Non-Stationary Stochastic Processes", CISM Advanced School on "Time and Frequency Representation of Signals and Systems", Udine, Italy, Sept. 1987.
2. W. Meclenbrauker, "Tutorial on Non-parametric Bilinear Time-Frequency Signal Representations", In Signal Processing, Les Houches Session XLV, Ed., J.L. Lacoume, T.S. Durrani,R.Stora, Elsevier Science Publ., 1987.
3. J. Proakis, Digital Communications, McGraw Hill, 1983.
4. B. Sankur, N.Tuğbay, Proc.3. Int.Symp.Computer and Information Sciences, pp.77-84, Izmir, 1988.
5. K.G.Beauchamp, Applications of Walsh and Related Functions, Academic Press, 1984.

Table-1:

	H(1,4)	H(1,7)	H(4,1)	H(7,1)
PAM (d=0.5T)	100	95	3	1
PAM (d=0.3T)	50	100	0	0
2-CPFSK (h=0.3)	1	0	59	100
2-CPFSK (h=0.5)	1	0	100	51
2-CPFSK (h=0.7)	-7	-2	41	-4

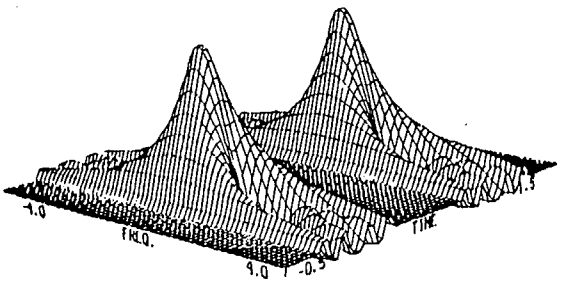

Figure-1: The WVD of PAM with BSS (d=T/2).

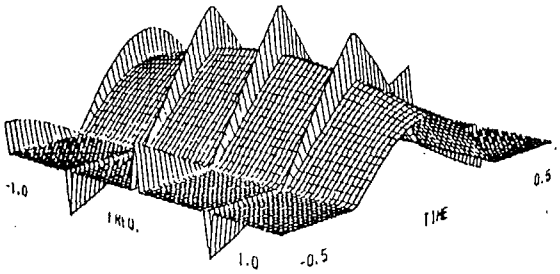

Figure-2: The WVD of PAM with OOS (d=T/2).

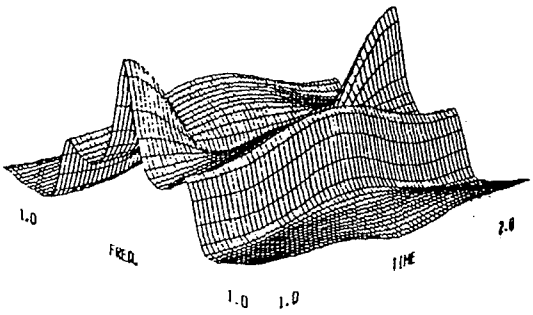

Figure-5: The WVD of 2-CPFSK with h=0.7.

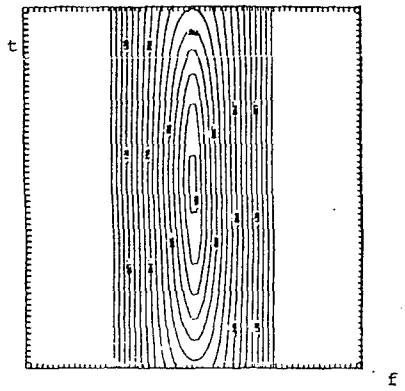

Figure-3: The isoplanars of the WVD of PAM with BSS (d=T/2).

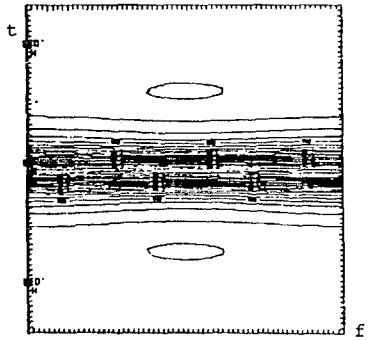

Figure-6: The isoplanars of the WVD of 2-CPFSK with h=0.3.

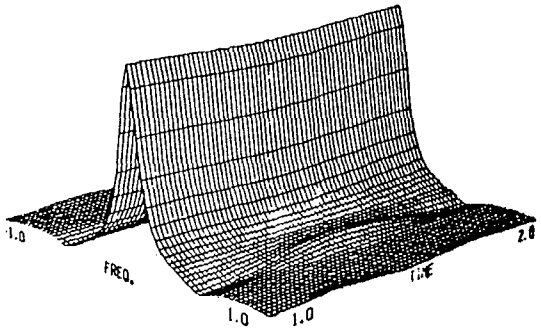

Figure-4: The WVD of 2-CPFSK with h=0.3.

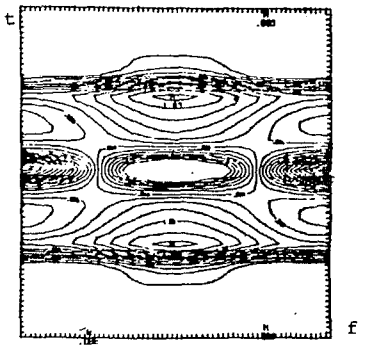

Figure-7: The isoplanars of the WVD of 2-CPFSK with h=0.7.

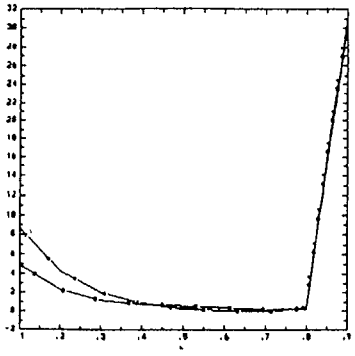

Figure-8: Variation of Haar coefficients with h.

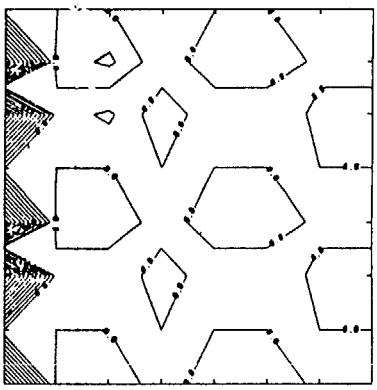

Figure-9: The isoplanars of Haar coefficients of the WVD for PAM with BSS (N=8).

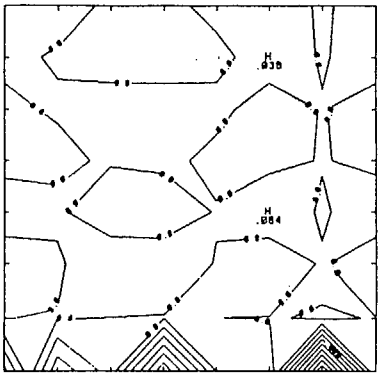

Figure-10: The isoplanars of Haar coefficients of the WVD for 2-CPFSK with h=0.3.

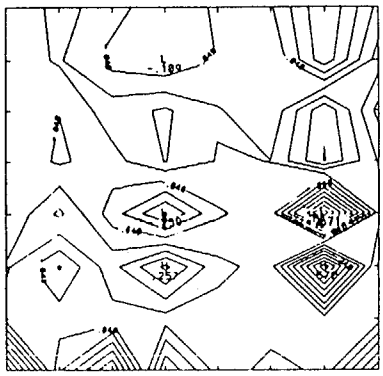

Figure-11: The isoplanars of Haar coefficients of the WVD for 2-CPFSK with h=0.7.